

# Kinetic aspects of self-discharge of nickel–hydrogen batteries and methods for its prevention

A. VISINTIN\*, A. ANANI<sup>†</sup>, S. SRINIVASAN, A. J. APPLEBY

*Center for Electrochemical Systems and Hydrogen Research, Texas Engineering Experiment Station, Texas A&M University, College Station, Texas 77843-3402 USA*

H. S. LIM

*Hughes Aircraft Company, Electron Dynamics Division, Torrance, CA 90505, USA*

Received 9 December 1992; revised 19 October 1994

Results of microcalorimetric experiments, in relation to self-discharge in Ni/H<sub>2</sub> batteries are reviewed; the mechanism of self-discharge, as well as possible methods for its inhibition, are discussed. These studies indicate that: (i) the self-discharge is due to a direct reaction of hydrogen with the charged active material (nickel oxide); (ii) the presence of metallic nickel sinter particles does not affect the reaction rate; (iii) the reaction rate depends linearly on hydrogen pressure indicating that the reaction is first order with respect to hydrogen; (iv) the reaction rate is higher under starved-electrolyte rather than flooded electrolyte conditions, indicating that the rate is affected by a diffusion process of dissolved hydrogen; and (v) the microcalorimetric heat evolution rate correlates with that of a decrease in electrode capacity due to the self-discharge reaction. The effects of additives to the active material of the nickel electrode were tested as an approach to reduction of the intrinsic rate of self-discharge. An alternate method for minimizing this rate is by storing the hydrogen as a hydride and thereby lowering the cell operating pressure. Some alloys were thus examined for their hydriding/dehydriding characteristics.

## 1. Introduction

The nickel-hydrogen (Ni/H<sub>2</sub>) battery is currently the most reliable secondary battery for space and other high power applications. An extremely long cycle life (up to 40 000 cycles at 80% depth of discharge) has been demonstrated [1]; its specific energy is approximately 40 Wh kg<sup>-1</sup> [2]. A Ni/H<sub>2</sub> battery can be overcharged for an extended period of time and overdischarged for a short duration without serious damage [3]. It also has the desirable feature of a built-in state-of-charge indicator for the cell pressure. The disadvantages of the Ni/H<sub>2</sub> battery are its relatively high self-discharge rate and low volumetric energy density, which thus makes it unsuitable for some applications. An understanding of the mechanism of the self-discharge reaction will be of value in attempts to minimize its rate. It is also necessary to investigate methods of increasing the volumetric energy density. The reaction of hydrogen with the charged active material (nickel oxide) of the nickel electrode controls the rate of self-discharge in the Ni/H<sub>2</sub> cell. At the typical operating pressures (30–50 atm), a Ni/H<sub>2</sub> cell will lose 50% of its capacity in approximately ten days at 20 °C [4]. According to some publications, the self-discharge rate of Ni/H<sub>2</sub>

cells is a first order chemical reaction with respect to hydrogen gas pressure [5, 6]. Another publication suggests that the self-discharge depends not only on hydrogen gas pressure but also on the amount of undercharged nickel oxyhydroxide [7]. Although the self-discharge rate can be reduced by lowering the cell operation pressure, this approach causes an increase in cell volume, and hence reduces the volumetric energy density of the cell. This option is thus not viable for many applications. The self-discharge reaction mechanism was previously investigated in our laboratory by microcalorimetry [8–10].

One approach to reduce the self-discharge rate, which is due to the intrinsic reaction between hydrogen and nickel oxyhydroxide (NiOOH), is by using additives to the electrode materials. Another approach is to lower the hydrogen pressure in the battery by using a hydrogen absorbing alloy. This approach was previously explored by using LaNi<sub>5</sub> as the hydrogen storage alloy in a Ni/H<sub>2</sub> cell [5, 11]. The alloy, LaNi<sub>5</sub>, has attractive absorption/desorption isotherm characteristics [12], but it presents some problems due to its long term chemical instability [11, 13], especially in a Ni/H<sub>2</sub> cell environment, and its mechanical instability during cycling [12]. Over 1000 charge/discharge cycles have been

\* Present Address: INIFTA-UNLP, C.C. 16, Sucursal 4, (1900) La Plata, Argentina.

<sup>†</sup> Present Address: Motorola, Energy Products Operations, 8000 West Sunrise Blvd., Plantation, FL 33322, USA.

demonstrated [14]. However, to determine the feasibility of this approach for a long-life application (such as for satellites), it is important to elucidate: (i) the discharge rate capability of the Ni/H<sub>2</sub> battery under reduced pressure conditions; (ii) the equilibrium hydrogen gas pressure and hydrogen absorption/desorption rate capability of hydride alloys (MH<sub>x</sub>); and (iii) the chemical stability of alloy material in the cell environment.

This paper presents the results of (a) microcalorimetric experiments to elucidate the self-discharge mechanism, (b) microcalorimetric studies of the self-discharge rates of nickel electrodes containing additives, and (c) a preliminary evaluation of hydrogen storage alloys to reduce the pressure of hydrogen in the Ni/H<sub>2</sub> battery.

## 2. Experimental details

Microcalorimetric experiments were carried out in a Hart Scientific model 5024 isotherm differential heat-conduction calorimeter with a noise-level below 0.3 μW, and a precision better than 1 μW. Temperature fluctuations of the water bath in the microcalorimeter were less than 0.0005 °C. Nickel oxide/oxyhydroxide electrodes, of the sintered type, were prepared by an electrochemical impregnation process, and contained cobalt as an additive (approximately 10%) in the active material [15], unless stated otherwise. Electrodes, with additives, were also prepared by an electrochemical impregnation using Ni(NO<sub>3</sub>)<sub>2</sub> electrolytes with the desired additives (approximately 2 M in total metal concentration) in a 1:1 ethanol-water solution. The impregnation was carried out at a current density of 93 mA cm<sup>-2</sup> for 2 h at or near the boiling point of the solution. The metal additive concentration ranged from 2.5 to 10% of total metal. Most samples had 10% Co in addition to other metallic additives, i.e., Fe, Cd, Mg, Sn, Bi and Pb. To produce the active material, the electrodes were subjected to four complete charge/discharge cycles in 20% KOH at a current density of 120 mA cm<sup>-2</sup>. Powder samples of β and γ-phase nickel oxides for the microcalorimetric studies were prepared from nickel electrodes, which were charged under different conditions [8, 9, 16], by grinding and magnetic separation of nickel metal from an aqueous slurry. The presence of β and γ-phases was confirmed by X-ray diffraction (XRD). Nickel metal powder samples were obtained by breaking up and grinding the nickel substrate.

The electrochemical cells consisted of a positive (nickel oxide/hydroxide) electrode, a negative (Pt catalysed hydrogen) electrode, a separator and a gas-screen, as previously described [9]. The nickel electrode area was 6.25 cm<sup>2</sup>. Nickel wires were spot welded to the electrodes for electrical connection. Before use, the nickel electrodes were cycled three times by charging at *C*/2 for 2 h and then discharging at the *C*/2 rate to -1.0 V against

Hg/HgO in 31% KOH solution. The electrode capacity was approximately 0.16 Ah.

The limiting discharge rate capability of a Ni/H<sub>2</sub> cell, under reduced cell pressure, was evaluated at various discharge rates and cell pressures using a 6 Ah boiler-plate cell, which was made of commercial space-cell quality electrodes and other cell components. The cell pressure was held at a constant value, during discharge, by connecting the cell to a large volume pressure chamber (about 100 times the cell void volume). Hydrogen absorption-desorption of the hydrogen storage alloys was measured using a modified version of Sievert's apparatus. Hydrogen absorption capacities of the alloys were calculated from the results of the isotherm measurements using the *P-V-T* relationship.

## 3. Results and discussion

### 3.1. Microcalorimetric studies

*3.1.1. Identification of self-discharge reaction.* To identify the self-discharge reaction in a Ni/H<sub>2</sub> cell, the rates of heat generation due to the reactions of hydrogen with various constituents of the nickel oxide electrode, (i.e., discharged active material (Ni(OH)<sub>2</sub>), charged active material (NiOOH), the metallic nickel substrate, and a combination of these), were investigated using the microcalorimetric technique. Typical experiments were carried out using approximately 0.2 g of sample in a sealed nickel tubular cell containing 0.5 cm<sup>3</sup> of 31% KOH electrolyte solution. Rates of heat evolution from the reactions of hydrogen with the charged active material (NiOOH), the metallic nickel substrate, and the nickel electrode, which contained both the active material and the substrate, respectively, are shown as a function of hydrogen pressure in Fig. 1. Each data point was taken after an 8 to 10 h reaction time

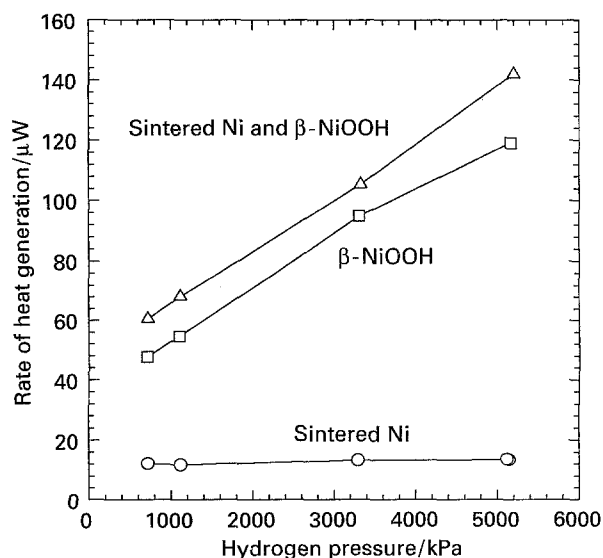


Fig. 1. Rate of heat generation of nickel hydroxide powders, and mixture of two powders as a function of hydrogen pressure in 31% KOH at 25 °C.

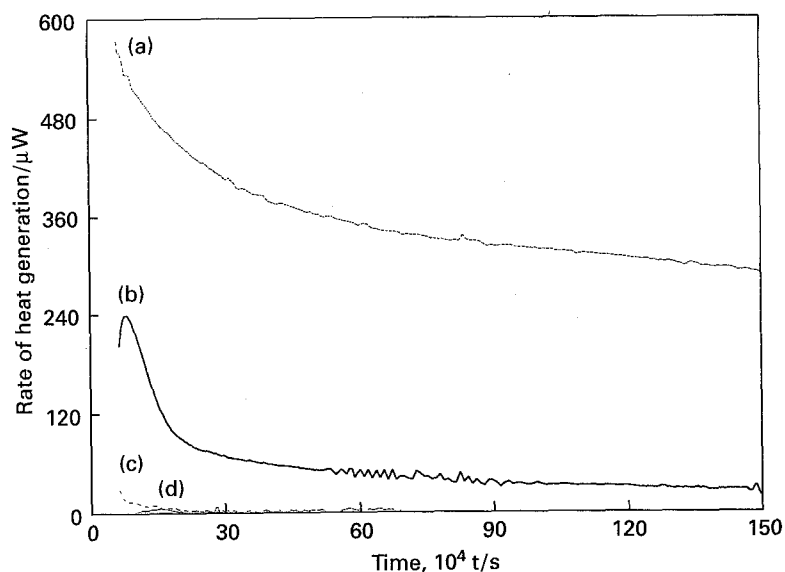


Fig. 2. Plots of heat evolution rates vs. the reaction time for (a) charged flight cell-type nickel electrode, (b) discharged flight cell-type nickel electrode, (c) a bare sintered nickel substrate material, (d) chemically prepared  $\text{Ni}(\text{OH})_2$ .

when a quasisteady state was reached. These results clearly indicate that the reaction rate of hydrogen with the metallic nickel substrate is negligible compared to that with  $\text{NiOOH}$ , or with  $\text{NiOOH}$  plus the substrate material [8, 9]. The difference in the rates of the latter two reactions was minor, indicating that the self-discharge reaction is due to the direct reaction of hydrogen with the charged active material ( $\text{NiOOH}$ ). The rate of heat evolution from the  $\text{NiOOH}$  powder increased roughly linearly with the hydrogen pressure over the range of 10 to 47 atm.

To eliminate the possibility of heat evolution from a reaction of the discharged active materials, microcalorimetric measurements were also performed using a discharged nickel electrode sample and also a chemically prepared nickel hydroxide ( $\beta\text{-Ni}(\text{OH})_2$ ). Heat evolution rates from these samples, at a hydrogen pressure of 47 atm at 25 °C, are compared with that for a charged electrode in Fig. 2. As expected, the heat evolution rate for the chemically prepared nickel hydroxide was negligible. The small amounts of heat from the electrochemically discharged electrode might be due to its incomplete discharge [17].

**3.1.2. Electrode heat evolution rate under flooded and starved electrolyte conditions.** To study the effects of diffusion of dissolved hydrogen in the electrolyte on the self-discharge rate, the microcalorimetric heat evolution rates from the electrodes were measured under various electrolytic conditions of the samples, as described below:

(a) *Flooded*: The electrode sample was fully immersed in the electrolyte in the microcalorimeter cell cavity.

(b) *Soaking wet*: Electrodes were presoaked in electrolyte, blotted with Whatman no. 40 filter paper to remove excess electrolyte and then a controlled amount (3 drops) of electrolyte was added to the microcalorimeter cell to make the sample ( $1.5\text{ cm}^2$ ) soaking-wet but not flooded.

(c) *Starved wet*: Similar to (b), but without addition of extra electrolyte after blotting.

(d) *Dried*: Sample in condition (a) was dried at 80 °C for 7 h (to a constant weight).

The effect of the above-mentioned electrolytic conditions on self-discharge rates, as measured by microcalorimetry at 47 atm of hydrogen pressure and at 25 °C, are shown in Fig. 3. The overall self-discharge is represented by:



The enthalpy change for this reaction is  $-144.85\text{ kJ mol}^{-1}$  at 25 °C [9, 18]. The capacity losses of the electrodes, due to the self-discharge reaction over a 24 h period, were determined to be approximately 3% under condition (a), 6% under (b), and over 12% under condition (c). These results indicate that the diffusion of dissolved hydrogen, in the electrolyte, towards the active material in the electrode partially limits the reaction rate. Under condition (a), the rate of heat evolution varied linearly with

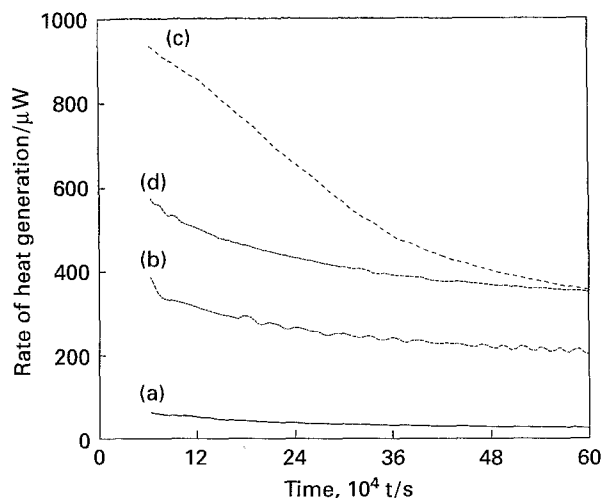


Fig. 3. Effects of the state of wetness (in 31% KOH) of an electrode on the heat evolution rate from flight cell-type nickel electrodes at a hydrogen pressure of 700 psig and 25 °C. Electrode area  $1.5\text{ cm}^2$ . (a) Flooded state, (b) fully wet state, (c) starved state, and (d) dried state.

hydrogen pressure, supporting the view that the reaction is diffusion-limited. The lower rates of heat evolution under condition (d), compared with condition (c), show that the presence of water accelerates self-discharge. The appreciable rate of heat evolution under condition (d) may still be due to traces of water in the extremely hygroscopic solid KOH.

**3.1.3. Effect of hydrogen pressure on rates of heat evolution and self-discharge.** Measurements were performed on the electrode in the 'starved wet' state (C). The extent of self-discharge was determined from the difference in the capacities of the electrode in the fully charged state and after it was subjected to the microcalorimetric experiments. The capacities were determined, in 31% KOH, by discharge at  $C/2$  to  $-1.0$  V vs Hg/HgO. The heat evolution rates due to self-discharge were recorded in the microcalorimeter over a period of two to three days. The procedure was carried out for different pressures using the same electrode samples, each of which had a capacity of about 40 mA h. Following these measurements, the electrodes were blotted with filter paper and placed in the microcalorimeter at a desired hydrogen pressure for an 8 and a 24 h monitoring of heat evolution. The remaining capacities were then measured, as described above. Figure 4 shows a log-log plot of the heat evolution rate against hydrogen pressure after 8 and 24 h periods. The slopes of the lines in

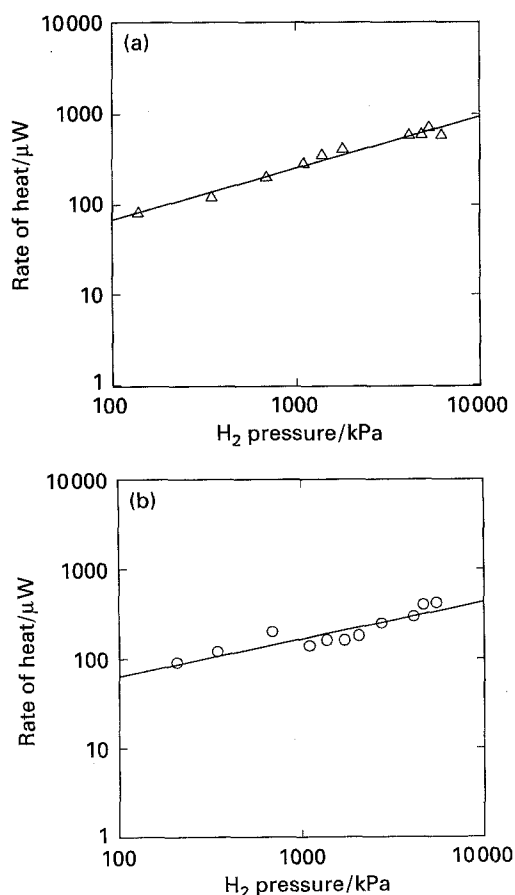
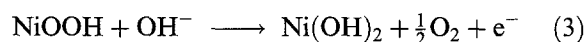


Fig. 4. Rate of heat generation after 8 h (a) and after 24 h (b) against pressure of hydrogen. Nickel oxyhydroxide containing 10% Co, electrode area  $1.5\text{ cm}^2$ , electrode dried with filter paper,  $25^\circ\text{C}$ .

Fig. 4 are almost identical, and have a value of 0.8. This value is reasonably close to unity, which is presumably the reaction order with respect to hydrogen. After an 8 h exposure of NiOOH to hydrogen, there is a deviation from this behaviour at higher pressure, leading to only a small effect of pressure on the heat evolution rate. However, after 24 h, a linear dependence occurs even at high pressures, but the line is shifted from that at lower pressures. There is no explanation for this behaviour at this time. The total heat generated in a 24 h period at different pressures was used to determine the rate of self-discharge, as represented by Reaction 1. The rates of self-discharge, as a function of pressure of hydrogen, estimated from measurements of the total heat generated and from the electrochemical capacity measurements before and after microcalorimetry, are in agreement as shown in Fig. 5. The results confirm our previous conclusions that the microcalorimetric technique is useful for determining self-discharge rates.

To determine the variation of heat evolution with hydrogen pressure, the activity of NiOOH must be maintained as close to unity as possible. This was achieved by using short exposure times of the sample to hydrogen. The experimental data of heat generation rate against pressure exhibit a linear behaviour, as seen in the regression fit in Fig. 6, only at lower hydrogen gas pressure. The intercept on the ordinate is not equal to zero, which probably is due to the decomposition of the higher oxides, according to the reactions:



The microcalorimetric technique is thus also useful in analysing the contributions of the reactions of higher

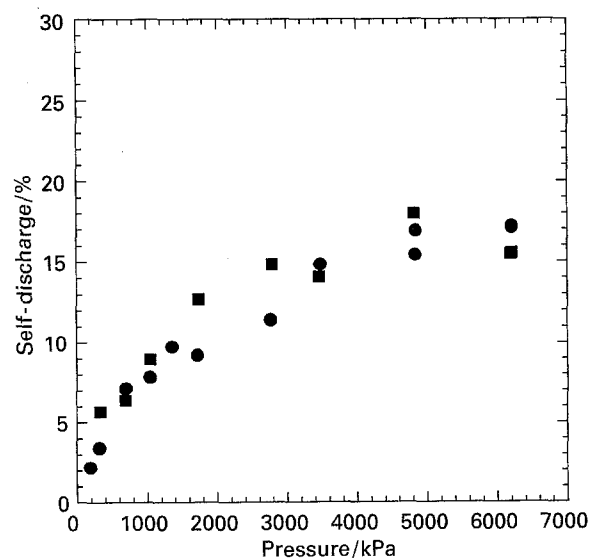


Fig. 5. Percentage of self-discharge, after 24 h, determined from (i) total heat generated (■) and (ii) the remaining capacity (●) as a function of hydrogen pressures. Nickel oxyhydroxide electrode containing 10% Co, electrode area  $1.5\text{ cm}^2$ , electrode dried with filter paper,  $25^\circ\text{C}$ .

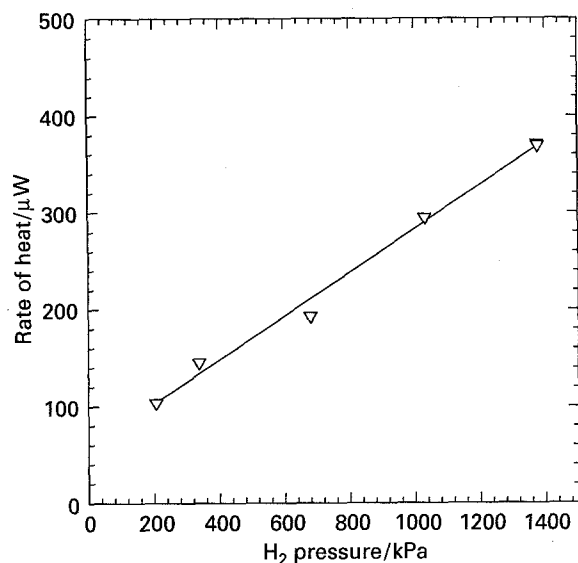


Fig. 6. Rate of heat generation after 3 h as a function of the hydrogen pressure for a nickel oxyhydroxide electrode containing 10% Co. Area of electrode:  $1.5\text{ cm}^2$ , electrode dried with filter paper,  $25^\circ\text{C}$ . Straight line is as expected from regression analysis.

nickel oxides (oxidation number  $>3$ ) to the overall heat evolution. Reactions 2 and 3 produce heat in the first few hours because of the electrodes being in an overcharged state. Such an explanation is validated by the results of capacity measurements, which show that the capacities of the electrodes in the absence of hydrogen gas are larger during the first two hours after overcharge, but remain constant over the next 24 h under open circuit conditions. For this reason, all initial capacity results discussed in this paper were measured 2 h after the end-of-charge.

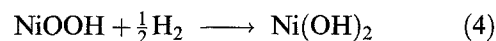
**3.1.4. Effect of the structure of nickel hydroxide on heat evolution rate.** The effect of the structure of NiOOH on the rate of heat evolution was investigated. A chemical procedure, by oxidation of nickel nitrate with  $\text{K}_2\text{S}_2\text{O}_8$  in KOH solution at room temperature, was used to prepare  $\beta$ -NiOOH. A sample of  $\gamma$ -NiOOH was obtained by direct oxidation of nickel nitrate with  $\text{Br}_2 + \text{NaOH}$  [9]. Both compounds were dried at  $80^\circ\text{C}$  for two days, and characterized by XRD. The  $\gamma$ -phase exhibited a higher rate of heat evolution than the  $\beta$ -phase. Nickel oxide electrodes were oxidized to the  $\gamma$ - or  $\beta$ -NiOOH state using the following procedures: (i) charging the electrode at the  $C/2$  rate for 4 h in 36% KOH to obtain  $\gamma$ -NiOOH as the predominant phase; and (ii) charging the electrode in 26% KOH electrolyte at the  $C/2$  rate for 2 h 20 min. to form the  $\beta$ -NiOOH. The electrodes were then cut to an area of  $1.5\text{ cm}^2$  before insertion into the microcalorimeter cell. The rate of heat evolution from the  $\gamma$ -phase was higher than that from the  $\beta$ -phase for these electrochemically-prepared samples, as was for the chemically-prepared materials.

Nickel oxyhydroxide ( $\text{NiOOH}\cdot 3\text{H}_2\text{O}$ ), purchased from Aldrich Chemical Company, was dried at  $120^\circ\text{C}$  for different periods of time to obtain samples with varying degrees of water of hydration. The

percentage of water removed was determined by weight loss. In one case, all hydrated water in the sample (37% by weight) was removed, while in another case only an equivalent of 20 wt% was removed. The partially dehydrated sample generated more heat than the fully dehydrated material, which was in turn higher than from the 'as-received' sample. Figure 7 shows the rate of heat evolution after 8 h and 24 h for a 0.2 g sample of the 'as-received' material as a function of hydrogen gas pressure. The slopes of these plots are close to 0.7, a value which is nearly the same as in the plots for the nickel oxyhydroxide electrodes (Fig. 4). The total heat generated in 24 h at different pressures was used to determine the rate of self-discharge assuming Reaction 1. The amount of self-discharge is again the same as that of the NiOOH electrode. This experiment demonstrates that the reduction of NiOOH takes place in the absence of electrolyte. These experiments provide evidence for the chemical reduction of NiOOH with hydrogen gas being the self-discharge reaction.

### 3.2. Heat evolution rate and self-discharge rate

Heat evolution rates due to the reaction of active NiOOH with hydrogen show a gradual decrease with time at a constant hydrogen gas pressure. This reflects the change of the amount of active material in the electrode as a function of time. Hence, self-discharge can be treated as a homogeneous chemical reaction, i.e.,



Assuming that the above reaction is first order with respect to NiOOH,

$$A = [A_0] e^{-kt} \quad (5)$$

where  $A$  is the activity of nickel oxyhydroxide and  $A_0$  is its value at time  $t = 0$ . It follows from Equation 5 that for a first order reaction  $[A]$  the heat evolution

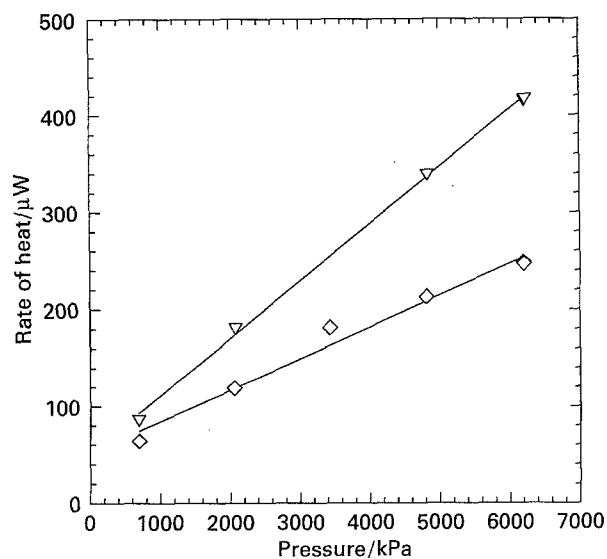


Fig. 7. Heat generation rates at 8 h ( $\nabla$ ) and 24 h ( $\diamond$ ) as a function of hydrogen pressure for 'as-received' nickel peroxide.

rate ( $J$ ), should decrease exponentially with time. Using the method of least squares, the experimental data fitted the equation:

$$f(t) = a + b e^{-ct} \quad (6)$$

where  $a$ ,  $b$  and  $c$  are constants,  $t$  is the time and  $f(t)$  represents the rate of generated heat. Figure 8(a)–(c) presents experimental results of the rate of heat generation against time for (a) chemically prepared  $\gamma$ -NiOOH (0.2 g, 56 mA h capacity), (b) an electrode prepared by electrochemical impregnation of a dry sinter, and (c) Aldrich nickel oxide hydrate (0.2 g). Also shown in these figures are the theoretical plots based on Equation 6, as well as of the differences between the experimental and theoretical plots. The results in Fig. 8(a) and (b) show excellent agreement between the experimental and fitted values, while the agreement is somewhat less satisfactory in Fig. 8(c).

### 3.3. Effect of additives on self-discharge rates

Additives to electrodes, tested in our laboratory, were Co, Cd, Fe, Mg, Zn, Pb, Bi and Sn. Calorimetric data from aerospace type nickel electrodes, containing various additives, including a combination of Co and

Cd, were summarized in previous publications [8, 10]. In this study additives were impregnated into the nickel oxide electrodes with cobalt (approximately 10%) by two different methods: (i) chemical precipitation using approximately 10 repeated immersions for 5 s each time in 2 M  $M(\text{NO}_3)_x$  ( $M = \text{Sn, Bi and Pb}$ ) and 31% KOH or (ii) cathodic electrodeposition in a  $M(\text{NO}_3)_x$  bath for 5 min at  $13 \text{ mA cm}^{-2}$ . The additives Bi, Sn or Cd appear to reduce the self-discharge rate by approximately 20%. However, these results demonstrate a relatively minor beneficial effect of these additives; further exploration of the additives for nickel oxide electrodes in Ni/H<sub>2</sub> cell does not seem warranted.

### 3.4. Studies on alloys for hydrogen storage

Another approach to reduction of the self-discharge rate of a Ni/H<sub>2</sub> cell is by use of a hydrogen absorbing alloy in the cell for hydrogen storage. The main objective of this approach is to reduce the operating pressure in the cell without changing the inherent characteristics of the electrochemical reactions. One of the critical cell characteristics in this approach is the discharge rate capability of the cell under reduced pressure. Discharge rates in a Ni/H<sub>2</sub> cell are limited by the rate of hydrogen supply to the negative electrode, and the purpose of this study was to evaluate such rates in cells using alloys for hydrogen storage at relatively low pressures.

**3.4.1. Limiting discharge rates of a Ni/H<sub>2</sub> cell at reduced H<sub>2</sub> pressures.** Discharge voltages of a boiler plate Ni/H<sub>2</sub> cell (6 Ah) at 4.55 A, from the 25% state of charge, were measured as a function of time at various pressures between 0.02 and 0.1 atm and at ambient temperature (20 °C). The cell voltages started to drop instantaneously when the cell pressure was 0.04 atm or below. But the voltages were sustained over 60 s when the pressure was 0.04 atm or above. Cell voltages, as a function of discharged amounts from a fully charged cell (during high current (10 to 50 A) discharges at 1 atm and ambient temperature) were compared with those in the conventional Ni/H<sub>2</sub> cell at an operating pressure (of 40 atm in the fully charged state). Cell voltages at the 50 A discharge rate were sustained at a useful voltage for only 10 to 15 s after which it started to drop rapidly. However, when the discharge current was lowered, for example to 30 to 40 A, the useful capacity was increased significantly. Cell voltages

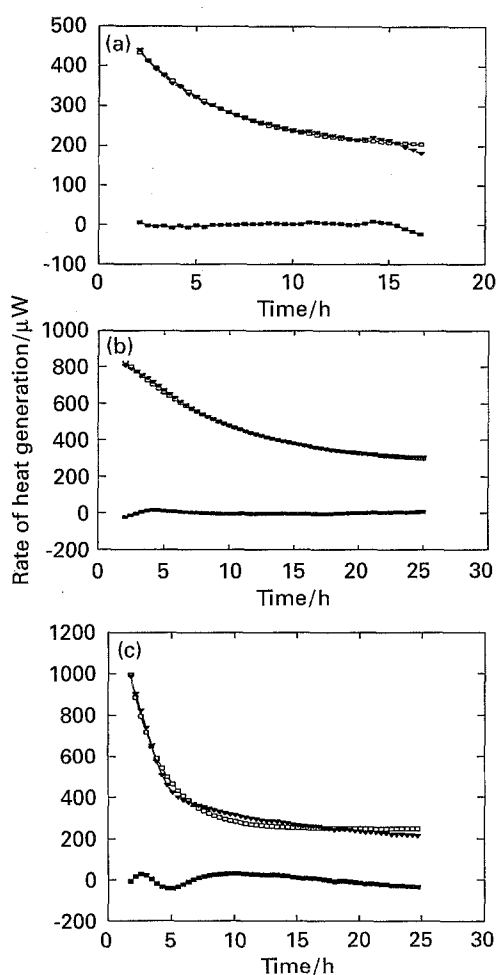


Fig. 8. Rate of heat generation as a function of time ( $\blacktriangle$ ), equation fitting ( $\square$ ), difference of theoretical and experimental data ( $\bullet$ ), at 700 psig of hydrogen. (a) 0.2 g  $\gamma$ -NiOOH powder, (b) nickel hydroxide electrode 10% Co, (c) 0.2 g 'as received' nickel peroxide material.

Table 1. Approximate values of limiting discharge rates of a 6 Ah Ni/H<sub>2</sub> cell at various H<sub>2</sub> pressures at 20 °C

H <sub>2</sub> pressure/atm	Approximate values of limiting discharge rates	
	Current/A	Discharge rate/ $\times C$
0.035	4.6	0.8
0.5	15–30	2.5–5.0
1.0	50	8.0

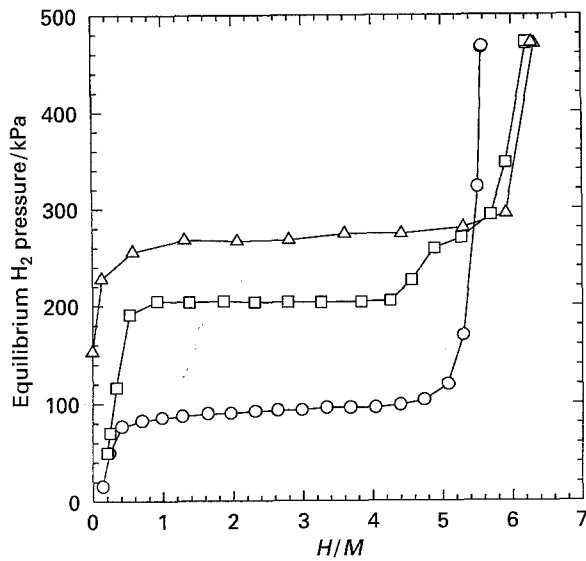


Fig. 9. Representative pressure-composition desorption isotherms for selected test hydrogen storage alloys BNL1; BNL3; at 25°C. Key: ( $\Delta$ ) LaNi<sub>5</sub>-Des-25, ( $\square$ ) BNL1-25 and ( $\circ$ ) BNL3-25-Des.

decreases were small at a 15 A discharge rate and at 0.5 and 1.35 atm.

Approximate values of the limiting discharge rates of the cell, at various hydrogen gas pressures, are estimated in Table 1. Limiting discharge rates appear to be roughly proportional to cell pressure. The present results indicate that if a device needs high power, for example, an 8C rate of discharge of the battery, the minimum operating pressure should be 1 atm and, therefore, the ideal plateau pressure of the isotherm of an alloy for hydrogen storage should be 1 atm or greater at ambient temperature. For a low temperature operation (say 10 °C), this plateau pressure at ambient temperature should be even higher than 1 atm because of the decrease in plateau pressure with temperature. The pressure values in the Table show an approximate guideline for the plateau pressure of the hydrogen storage alloy.

3.4.2. *Hydrogen storage alloys.* The pressure of the state-of-the-art Ni/H<sub>2</sub> battery could be as high as 70 atm when it is fully charged. Thus, in Fig. 5, it is clear that the self-discharge rate for this battery will be quite high. Many alloys absorb hydrogen reversibly. However, constraints imposed by the

Ni/H<sub>2</sub> cell environment restrict the choice of possible candidates. Desired alloy properties are (i) high hydrogen absorption capacity using long-term cycling, (ii) plateau pressure of about 1 atm at room temperature, and (iii) good chemical stability in the battery environment. The pressure-composition isotherms for several AB<sub>5</sub> type alloys have been determined in our laboratory [19]. Figure 9 shows a family of desorption isotherms at 25 °C for selected alloys (AB<sub>5</sub> and some new compositions). The hydrogen absorption/desorption capacity may be calculated using the ideal gas *P-C-T* relationship. The usable hydrogen storage (*C*) capacity, expressed in electrochemical terms (mA h g<sup>-1</sup>) for these alloys, could be calculated using the following equation:

$$C = (2.68 \times 10^4 / M)(H_{p5} - H_{p0.5}) \text{ mA h g}^{-1} \quad (7)$$

where H<sub>p5</sub> and H<sub>p0.5</sub> are the hydrogen content per mole in the pressure-composition isotherms at pressure of 5 and 0.5 atm, respectively, and *M* is the molecular weight of the alloy. Capacities and other storage properties for the investigated alloys are compared with that for LaNi<sub>5</sub>, in Table 2. Two new compositions ('BNL1' and 'BNL3') showed lower equilibrium dissociation pressures than that for LaNi<sub>5</sub>, because of the incorporation of cobalt and/or tin additives.

4. Conclusions

The microcalorimetric results reveal that (i) the self-discharge is due to a direct reaction of hydrogen with the charged active material (nickel oxide), (ii) the presence of sintered nickel particles did not affect the reaction rate, (iii) the reaction rate varies linearly with hydrogen pressure, indicating that the reaction is first order with respect to hydrogen, (iv) the reaction rate was higher under a starved-electrolyte condition than under a flooded condition, suggesting that the rate is determined by diffusion of the dissolved hydrogen in the electrolyte, and (v) the microcalorimetric heat generation rate correlates with the rate of decrease of electrode capacity caused by the self-discharge reaction. Of all the tested additives to the nickel oxide electrode, combinations of Bi, Sn and Cd with Co appear to be most effective

Table 2. Characteristics of hydrogen storage in select alloys

Alloy composition	Plateau pressure /atm	Hydrogen content at		H <sub>2</sub> capacity /mA h g <sup>-1</sup>
		P = 0.5 atm	P = 5.0 atm	
		H/mol		
LaNi <sub>5</sub>	2.5 to 3.3	0.00	6.02	372
	2.4 to 2.8	0.00	6.31	
BNL1	2.44	0.04	6.2	354
	2.00	0.2	6.2	
BNL3	1.08	0.29	5.92	335
	0.96	0.3	5.60	
BNL4	<0.70	-	~90.0	402

The first and second rows of numbers along each sample represent absorption and desorption measurements, respectively.

in reducing self-discharge rate. The discharge rates of a Ni/H<sub>2</sub> cell were determined as a function of hydrogen pressure, at rates as high as 8C. A pressure of at least 1 atm of hydrogen is required for discharge at such high rates. Thus, if alloys are to be used for hydrogen storage as hydrides, the plateau pressures of these alloys for hydrogen desorption at ambient temperature will have to be about 1 atm. The alloys ('BNL1' and 'BNL3' (see Table 2) show desirable thermodynamic properties, as hydrogen storage materials, to lower the pressure in Ni/H<sub>2</sub> batteries.

### Acknowledgements

This work was sponsored by Hughes Aircraft Company (Contract 88 (44) 000281/66525), and the NASA Center for Space Power at Texas A&M University (Contract P.O. 58-529211-X 113). Dr Arnaldo Visintin was at TAMU on an International Exchange Program under the auspices of the federal agencies CONICET (Argentina) and NSF (USA). The authors also wish to thank Dr M. P. Sridhar Kumar for his help in the final editing of this manuscript.

### References

- [1] H. S. Lim and S. A. Verzwylt, *J. Power Sources* **22** (1988) 213; *ibid.* **29** (1990) 503.
- [2] E. Adler and F. A. Perez, Proceedings of the 21st Intersociety Energy Conversion Engineering Conference, **3** (1986) p. 1554.
- [3] H. S. Lim and S. J. Stadnick, *J. Power Sources* **27** (1989) 69.
- [4] J. F. Stockel, Proceedings of the 20th Intersociety Energy Conversion Engineering Conference, **1** (1985) p. 171.
- [5] G. Holleck, Proceedings of GSFC Battery Workshop, NASA CP-2041 (1977) p. 525-31.
- [6] P. F. Ritterman and A. M. King, Proceedings of the 20th Intersociety Energy Conversion Engineering Conference, **1** (1985) p. 175.
- [7] B. I. Tsenter and A. I. Sluzhevskii, *Electrokhimiya* **54** (1980) 2545.
- [8] A. Visintin, S. Srinivasan, A. J. Appleby and H. S. Lim, *J. Electrochem. Soc.* **139** (1992) 985.
- [9] Y. J. Kim, A. Visintin, S. Srinivasan and A. J. Appleby, *ibid.* **139** (1992) 351.
- [10] Z. Mao, A. Visintin, S. Srinivasan, A. J. Appleby and H. S. Lim, *J. Appl. Electrochem.* **22** (1992) 409.
- [11] G. L. Holleck, J. R. Driscoll and B. E. Paul, *J. Less-Common Metals* **74** (1980) 379.
- [12] J. J. G. Willems, *Philips J. Res.* **39**, Suppl. no. 1, (1984) 1-94.
- [13] G. D. Sandrock and P. D. Goodell, *J. Less-Common Metals* **104** (1984) 159.
- [14] H. F. Bittner and M. V. Quinzio, Proceedings of the 20th Intersociety Energy Conversion Engineering Conference, **1** (1985) p. 163.
- [15] D. F. Pickett and J. T. Malloy, *J. Electrochem. Soc.* **125** (1978) 1026.
- [16] J. P. Harivel, B. Morignat, J. Labat and J. F. Lauret, 'Power Sources', (edited by D. H. Collins), Pergamon Press, Oxford (1966) p. 239.
- [17] C. Dyer, in 'The Nickel Electrode', (edited by G. R. Gunther and S. Gross), Symposium volume, The Electrochemical Society, Pennington, NJ (1982) p. 119.
- [18] S. G. Bratsh, *J. Phys. Chem. Data* **18** (1989) 1.
- [19] A. Anani, A. Visintin, K. Petrov, S. Srinivasan, J. Reilly, J. Johnson, R. Schwarz and P. Desch, *J. Power Sources* **47** (1994) 261.